ACS OMEGA

Article

Cite This: ACS Omega 2018, 3, 14423−14430

http://pubs.acs.org/journal/acsodf

# Evidence for the Superatom−Superatom Bonding from Bond Energies

Qijian Zheng,[†] Chang Xu,*[,†] Xia Wu,*[,§] and Longjiu Cheng*[,†,‡]

[†]Department of Chemistry, Anhui University, Hefei, Anhui 230601, People's Republic of China

[‡]AnHui Province Key Laboratory of Chemistry for Inorganic/Organic Hybrid Functionalized Materials, Anhui University, Hefei, Anhui 230601, P. R. China

[§]AnHui Province Key Laboratory of Optoelectronic and Magnetism Functional Materials, School of Chemistry and Chemical Engineering, Anqing Normal University, Anqing 246011, PR China

**ABSTRACT:** Metal clusters with specific number of valence electrons are described as superatoms. Super valence bond (SVB) model points out that superatoms could form the superatomic molecules through SVBs by sharing nucleus and electrons. The existence of superatom−superatom bonding was verified by the shape of their orbitals in former studies. In this paper, another important evidence—bond energy is studied as the criterion for the SVBs using the density functional theory method. In order to get the reliable values of bond energies, the series of Zn−Cu and Mg−Li superatomic molecules composed of two tetrahedral superatoms which do not share their nucleus are designed. Considering the number of the valence electrons in one tetrahedral superatomic unit, $(Zn_4)_2/(Mg_4)_2$, $(Zn_3Cu)_2/(Mg_3Li)_2$, $(Zn_2Cu_2)_2/(Mg_2Li_2)_2$, and $(ZnCu_3)_2/(MgLi_3)_2$ clusters are 8e−8e, 7e−7e, 6e−6e, and 5e−5e binary superatomic molecules with super nonbond, single bond, double bond, and triple bond, respectively, which are verified by chemical bonding analysis depending on the SVB model. Further calculations reveal that the bond energies increase and the bond lengths decrease along with the bond orders in Zn−Cu and Mg−Li systems which is in accordance with the classical nonbond, single bond, double bond, and triple bond in C−H systems. Thus, these values of bond energies confirm the existence of the SVBs. Moreover, electron localization function analysis is also carried on to describe the similarity between the superatomic bonds and atomic bonds in simple molecules directly. This study reveals the new evidence for the existence of the superatom−superatom bonding depending on the bond energies, which gives the new insight for the further investigation of the superatomic clusters.

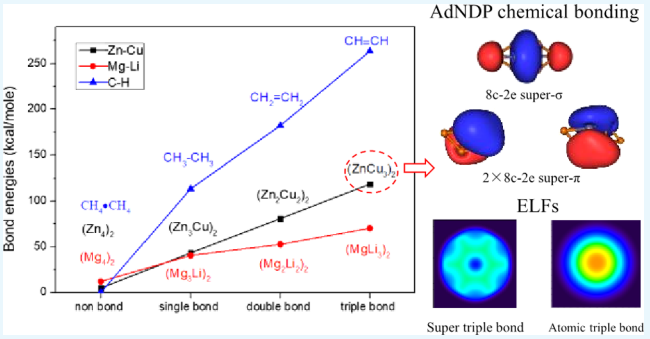


## 1. INTRODUCTION

The metal clusters with specific valence electrons could be described by a nearly confined free electron gas in a spherically symmetric potential which is defined as the spherical shell Jellium model,[1−8] and these novel clusters are named as the superatoms.[9−20] The electronic states in superatoms are proposed to bunch into several superatomic orbitals of $|1s^2|1p^6|1d^{10}|2s^21f^{14}|2p^61g^{18}|2d^{10}3s^21h^{22}|$..., where the resulting magic numbers are 2, 8, 18, 20, 34, 40, 58, 68, and 90... This theory of superatom has achieved great success in discussing the electronic structures of spherical metal clusters.[21−27] Taking the $Al_{13}^-$ cluster as an example, it could be viewed as a superatom with an icosahedral motif, which has the closed electronic shell with 40 valence electrons ($|1s^2|1p^6|1d^{10}|2s^21f^{14}|2p^6|$).[28−33] However, this model meets some difficulties when discussing the clusters with a nonspherical structure. In 2013, Cheng and Yang[34] proposed the super valence bond (SVB) model, which gives the new insight into the electronic structure of superatomic clusters. In this model, a prolate cluster is divided into two spherical blocks sharing nucleus and valence pairs to achieve electronic closed shell.[35−41] This bonding pattern between superatoms is defined as the SVB which has the similar characteristics as the bonding pattern between simple atoms.

The SVB model has been successfully applied in understanding the electronic structures of variety superatomic clusters, especially in some nonspherical clusters. For example, the prolate double-core $Li_{14}$ could be viewed as the union of two 10c−7e (ten-center seven-electron) spherical superatoms sharing a six-nucleus octahedron, which is the analogues of $F_2$ with the single covalent bond.[34] Another example is $Li_{20}Mg_3$ (26 super valance electrons), it is formed by two 13c−13e (thirteen-center thirteen-electron) superatoms and has the similar electronic structure as $V_2$, where the super quintuple bonding exists.[36] In addition to the super covalent bonds between superatoms, the superatomic orbitals could also

Received: July 31, 2018
Accepted: October 18, 2018
Published: October 31, 2018

hybridize to form the super hybrid bonds in the ligand field.[34,42,43] The super orbitals of the $Au_6$ core in the ligand-protected gold clusters could compose the $sp^3$, $sp^2$ and, sp hybrid to interact with the peripheral atoms to form the super hybrid bonds, which are similar as $CH_4$, $NH_3$, and $H_2O$ molecules with tetrahedral, trigonal pyramidal, and angular shapes.[44,45] Moreover, the $sp^2$ $Au_6$ superatomic unit could compose the $Au_{42}$ cluster with $\pi$ aromaticity.[46] Another example is the $Au_{20}$ cluster, in which the superatomic orbital of the truncated tetrahedron $Au_{16}$ core undergo the $d^3s$ hybridization to interact with the four apical Au atoms.[47−51] A recent study reveals the 8e ligand-protected $[Au_{12}(SR)_6]_2$ cluster with the $sp^3$ core, which exhibits the special bonding and optical properties.[52]

The SVB model reveals various bonding patterns between superatoms depending on the shape of orbitals. However, bond energy corresponding to the bond order is another key parameter for chemical bonding which has not been discussed for superatomic molecules before. In this paper, bond energies between superatoms are calculated and compared with the atomic bonds to verify the existence of SVBs. As the bond energies between superatoms sharing nucleus are hard to evaluate in the superatomic molecule, we design a series of Zn−Cu and Mg−Li metal clusters composed of two tetrahedral superatoms in which superatoms are just sharing electrons to form the SVB for our study. AdNDP (adaptive natural density partitioning) chemical bondings are investigated to reveal the superatomic bonding patterns in these superatomic molecules. The calculated bond energies of the superatomic bonds are compared with the nonbond, single bond, double bond, and triple bond between simple atoms. Further electron localization function (ELF) analysis is carried out to ensure the existence of these kind of SVBs from the strength of the electronic interaction.

## 2. RESULTS AND DISCUSSION

**2.1. Geometric Modeling.** The superatoms with the tetrahedral structure are popular in ligand-protected metal clusters,[48,53−60] such as $(Au_6)$ the core of $[Au_6(Ni_3(CO)_6)_4]^{2-}$ cluster,[44] and $(Ag_4)$ core in $Ag_4X_4$ (X = H, Li, Na, K, Cu, Ag, Au, and F, Cl, Br) clusters.[61] Therefore, two tetrahedral 8e superatoms $Zn_4$ and $Mg_4$ with the electronic shell filled as $|1s^2|1p^6|$ are chosen as the objects in our study. Take the $Zn_4$ cluster as the example, two $Zn_4$ superatom compose the prolate $(Zn_4)_2$ superatomic molecule, then Zn atoms in contraposition of two separate units are gradually replaced by Cu atoms with one less valence electron and the similar electronegativity, in order to obtain the superatomic molecules of $(Zn_3Cu)_2$, $(Zn_2Cu_2)_2$, and $(ZnCu_3)_2$ with the different valence electrons. All the structures are optimized at the PBE0/def2-tzvp level of theory, and the optimized structures are plotted in Figure 1a−e. As shown in Figure 1a, $Zn_4$ is a $T_d$ superatom with the large highest occupied molecular orbital−lowest unoccupied molecular orbital (HOMO−LUMO) energy gap of 4.12 eV. The $(Zn_4)_2$ cluster composed of two $Zn_4$ units in Figure 2b has the $D_{3d}$ symmetry and the HOMO−LUMO gap of 2.96 eV. In Figure 1c, two vertex atoms of the $(Zn_4)_2$ cluster are replaced by Cu to form the $D_{3d}$ $(Zn_3Cu)_2$ cluster in order to ensure that the electronic density is more concentrated in the waist of the cluster which indicates a strong interaction. This cluster has a more compact structure compared to $(Zn_4)_2$ and the large HOMO−LUMO gap of 2.65 eV. When another two Zn atoms in contraposition of the cluster are replaced by Cu, the

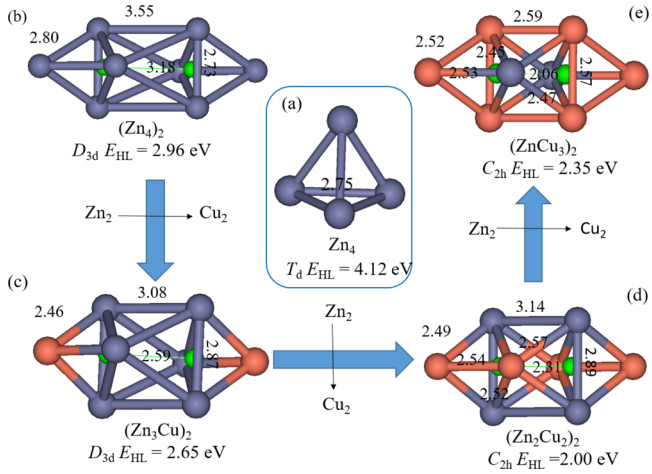


**Figure 1.** Optimized structures of Zn−Cu binary clusters (Zn-blue, Cu-orange) at the PBE0/def2-tzvp level of theory. The symmetries, HOMO−LUMO energy gaps, bond lengths and the distances between the centers (labeled green) in back faces of two tetrahedral units in Angstrom (Å) are labeled.

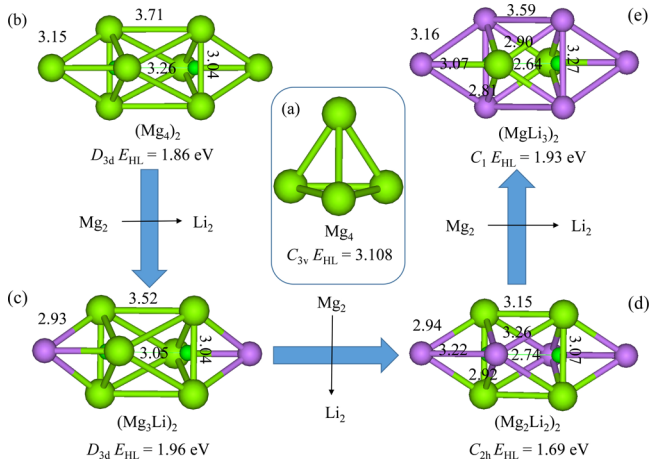


**Figure 2.** Optimized structures of Mg−Li binary clusters (Mg-green, Li-purple) at the PBE0/def2-tzvp level of theory. The symmetries, HOMO−LUMO energy gaps, bond lengths, and the distances between the centers (labeled green) in back faces of two tetrahedral units in Angstrom (Å) are labeled.

$(Zn_2Cu_2)_2$ cluster gets a better symmetry of $C_{2h}$ and the HOMO−LUMO gap of 2.00 eV, of which the triplet state is more stable. Finally, the $(ZnCu_3)_2$ cluster is obtained by replacing the other two Zn atoms by Cu. This cluster has the $C_{2h}$ symmetry with HOMO−LUMO gap of 2.35 eV. Moreover, the bond lengths and the distances between the centers in back faces of two tetrahedral units for each structure are also labeled in the Figure 1. The structures of this series of clusters are becoming more compact from Figure 1b−e as their bond lengths and face−face distances are getting smaller, which indicates the increasing Zn−Cu interaction. The Mg−Li binary clusters undergo the similar structural evolution as the Mg atoms are gradually replaced by Li atoms, as shown in Figure 2.

**2.2. Chemical Bonding Analysis.** As mentioned above, $Zn_4$ cluster could be viewed as the superatom of the 8e close shell electronic structure. Thus, it could be inferred that $(Zn_4)_2$ is composed of two $Zn_4$ superatoms through the 8e−8e super nonbond. As the Cu atom has one less valence electron than



DOI: 10.1021/acsomega.8b01841
ACS Omega 2018, 3, 14423−14430

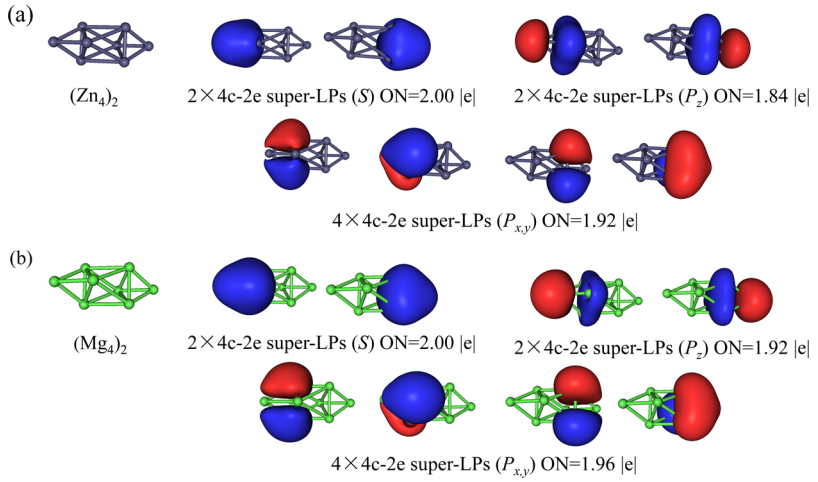


**Figure 3.** Geometric structures and AdNDP chemical bodings of (a) $(Zn_4)_2$ and (b) $(Mg_4)_2$. Occupied numbers are labeled below the structures.

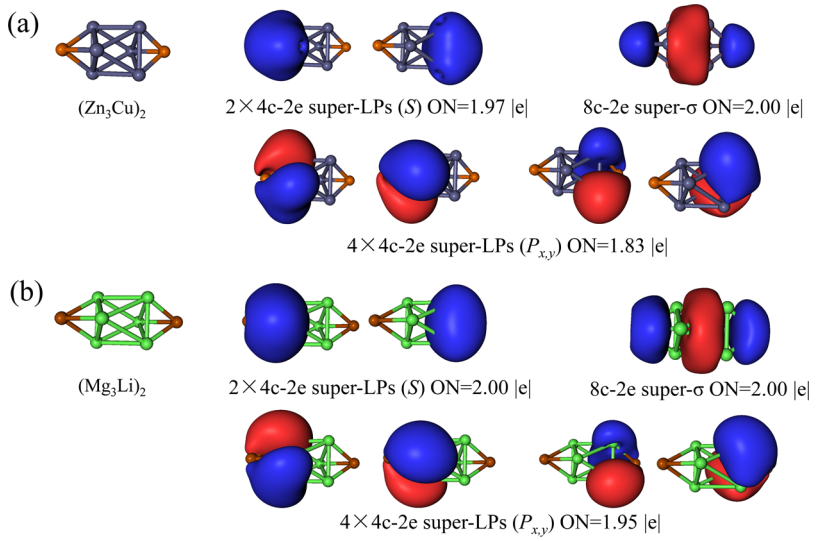


**Figure 4.** Geometric structures and AdNDP chemical bodings of (a) $(Zn_3Cu)_2$ and (b) $(Mg_3Li)_2$. Occupied numbers are labeled below the structures.

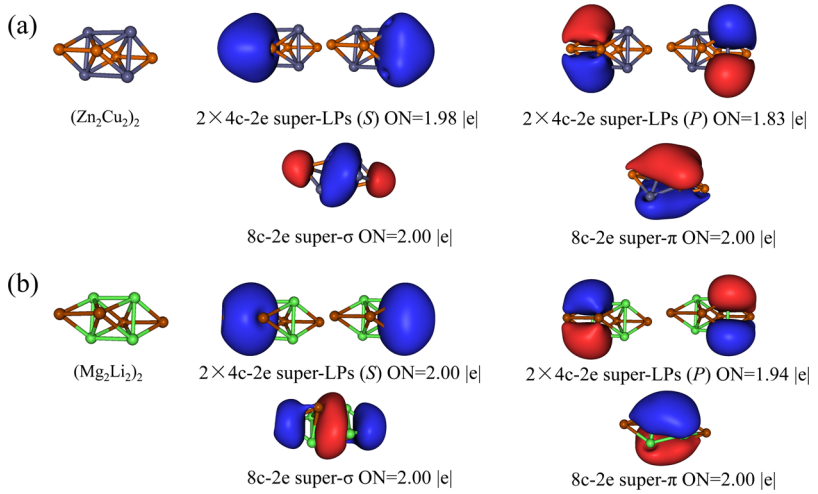


**Figure 5.** Geometric structures and AdNDP chemical bodings of (a) $(Zn_2Cu_2)_2$ and (b) $(Mg_2Li_2)_2$. Occupied numbers are labeled below the structures.

Zn, $(Zn_3Cu)$ unit could be viewed as a 7e superatom, which would form the single SVB when composing the $(Zn_3Cu)_2$ cluster. Similarly, $(Zn_2Cu_2)_2$ is composed of two 6e $(Zn_2Cu_2)$ units through the double SVB, and $(ZnCu_3)_2$ is formed by two



DOI: 10.1021/acsomega.8b01841
*ACS Omega* 2018, 3, 14423−14430

5e ($ZnCu_3$) units through the triple SVB. The Mg−Li binary clusters would follow the similar rule in their chemical bonding systems. In order to verify our inference, electronic characters of these clusters are discussed depending on the SVB model using the AdNDP method. This method was developed by Zubarev and Boldyrev[62−65] and wildly used to analyze the multicenter bonding systems in carbon, boron, and metal clusters.

As shown in Figure 3, AdNDP analysis reveals that there are four 4c−2e super lone pairs (LPs) in each tetrahedral $Zn_4/Mg_4$ unit with ON (occupied number) = 2.00 |e| (s), 1.92 |e| ($p_{x,y}$), 1.84 |e| ($p_z$) in $(Zn_4)_2$, and 2.00 |e| (s), 1.96 |e| ($p_{x,y}$), 1.92 |e| ($p_z$) in $(Mg_4)_2$. Therefore, the $Zn_4/Mg_4$ unit could be viewed as the 4c−8e superatom, which form the $(Zn_4)_2/(Mg_4)_2$ superatomic molecule through the 8e−8e super nonbond just as two inert gas atoms or two $CH_4$ molecules.

In Figure 4a, $(Zn_3Cu)_2$ could be viewed as the union of two 4c−7e ($Zn_3Cu$) superatoms. AdNDP analysis reveals that there are three 4c−2e super LPs in each ($Zn_3Cu$) unit (ON = 1.97 |e| for s, 1.83 |e| for $p_{x,y}$) and one 8c−2e $p_z$−$p_z$ $\sigma$ bond between two ($Zn_3Cu$) units (ON = 2.00 |e|). The $(Mg_3Li)_2$ also has three LPs at each side of the superatomic molecule (ON = 2.00 |e| for s, and 1.95 |e| for $p_{x,y}$) and one 8c−2e $p_z$−$p_z$ $\sigma$ bonds (ON = 2.00 |e|), as shown in Figure 4b. These clusters have the similar bonding pattern as $F_2$ and $CH_3$−$CH_3$ molecules and the $Li_{14}$ superatomic molecule,[34] which indicate the existence of a super single bond.

The AdNDP chemical bondings of $(Zn_2Cu_2)_2$ are shown in Figure 5a. The result indicates that there are two 4c−2e LPs (s, $p_x$) in each ($Zn_2Cu_2$) unit with ON = 1.98 |e|, 1.83 |e|, respectively. Moreover, the other p orbitals of two ($Zn_2Cu_2$) units form the 8c−2e $p_z$−$p_z$ $\sigma$ bond and $p_y$−$p_y$ $\pi$ bond with ON = 2.00 |e|. Similarly, the $(Mg_2Li_2)_2$ also has two LPs at each side of the superatomic molecule (ON = 2.00 |e| for s, and 1.94 |e| for $p_x$) and two 8c−2e bonds ($p_z$−$p_z$ $\sigma$, $p_y$−$p_y$ $\pi$) (ON = 2.00 |e|), as shown in Figure 5b. These clusters have the similar bonding pattern as $O_2$ and $CH_2$=$CH_2$ molecules, which could be viewed as the super double bond.

As shown in Figure 6a, there is one 4c−2e LP (s) in each ($ZnCu_3$) unit with ON = 1.96 |e|. The p orbitals in two ($ZnCu_3$) units of the $(ZnCu_3)_2$ cluster form one 8c−2e $p_z$−$p_z$ $\sigma$ bond and two 8c−2e $\pi$ bonds ($p_x$−$p_x$, $p_y$−$p_y$) with ON = 2.00 |e|. $(LiMg_3)_2$ also has one LPs at each side of the superatomic molecule (ON = 1.99 |e|) and three 8c−2e bonds ($\sigma$, 2$\pi$) (ON = 2.00 |e|), as shown in Figure 6b. These clusters have the similar bonding pattern as $N_2$ and CH≡CH molecules, which could be viewed as the super triple bond.

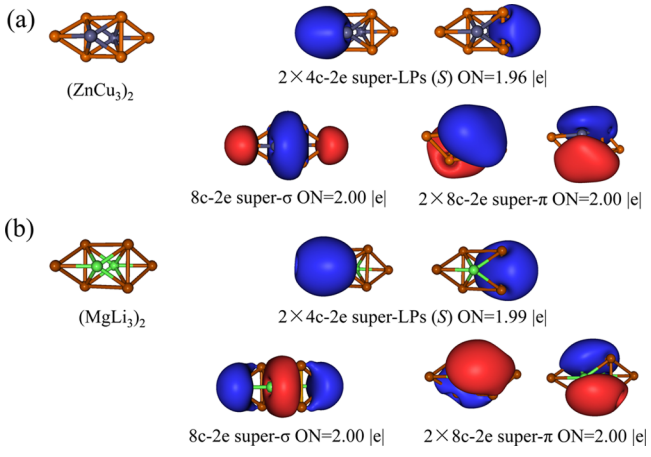


**Figure 6.** Geometric structures and AdNDP chemical bodings of (a) $(ZnCu_3)_2$ and (b) $(MgLi_3)_2$. Occupied numbers are labeled below the structures.

**2.3. Comparison of Bond Energies.** AdNDP chemical bonding analysis verifies that non bond, single bond, double bond and triple bond have also existed in the superatomic molecules depending on the SVB model. Furthermore, bond energy is another key parameter for chemical bonding. Thus, the bond energies of these super non bond, single bond, double bond and triple bond are calculated and compared with the corresponding atomic bonds in the following part.

As these superatomic molecules are formed by the two tetrahedral superatomic units which do not share the atomic nucleus, their bond energy is defined as $E_b$(superatomic molecule) = $E$(superatomic molecule) − 2$E$(superatoms) in our discussions, such as $E_b(Zn_4)_2 = E((Zn_4)_2) - 2E(Zn_4)$. The bond energies for Zn−Cu, and Mg−Li systems with different superatomic bond orders and their variation trend are obtained in Figure 7. Moreover, the bond energies of the classical nonbond, single bond, double bond, and triple bond in C−H systems of $CH_4$·$CH_4$, $CH_3$−$CH_3$, $CH_2$=$CH_2$ and CH≡CH molecules are also calculated for comparison.

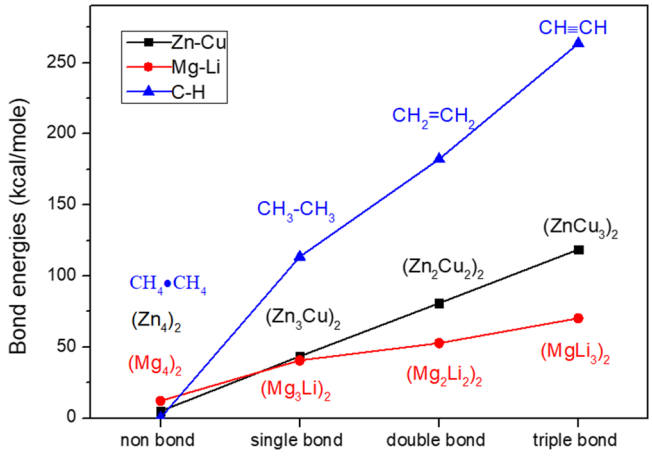


**Figure 7.** Bond energies vs bonder orders in C−H, Zn−Cu, and Mg−Li systems.

As shown in Figure 7, the bond energies in Zn−Cu/Mg−Li superatomic molecules gradually increase along with their bond orders, which is similar as hydrocarbon molecules. Thus, the superatomic bonds are getting more intense from nonbond to triple bond, but still a little weaker than the corresponding atomic bonds. This similar variation trend between the molecules and superatomic molecules indicates their similar bonding characters, which confirm the existence of the super nonbond, single bond, double bond, and triple bond. Moreover, by comparing Zn−Cu with Mg−Li systems, we found that their bond energies are almost the same in single bond ($\sigma$ bond) systems, whereas in double and triple bond ($\sigma$ + $\pi$, $\sigma$ + 2$\pi$) systems the differences increase. Thus, the differences of bond energies are derived from the delocalized $\pi$ bonds, which are stronger in Zn−Cu systems probably because of their more compact geometric structures and Cu−Cu metallophilic interaction.

Furthermore, in order to compare the detailed characteristics of super nonbond, single bond, double bond, and triple



DOI: 10.1021/acsomega.8b01841
ACS Omega 2018, 3, 14423−14430

bond, the variation trends of bond energies versus the face−face distance between two tetrahedral units in Zn−Cu and Mg−Li systems with different bond orders are calculated respectively. The lowest point in the energy curve represents the equilibrium structure of the cluster, of which the corresponding R (face−face distance) is the bond length. The result in Figure 8 indicates that the bond lengths decrease

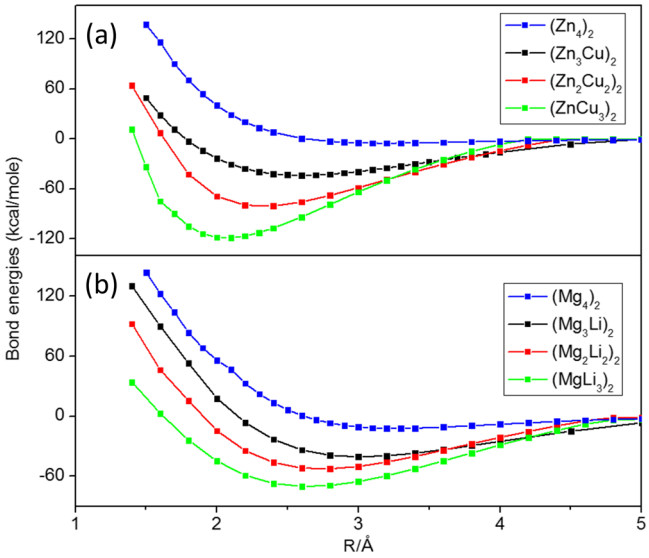


**Figure 8.** Variation trend of bond energies vs the face−face distance between two tetrahedral units in (a) Zn−Cu and (b) Mg−Li systems, respectively.

and the bond energies increases along with the bond orders, which is in accordance with the classical atomic non bond, single bond, double bond, and triple bond.

**2.4. Electron Localization Functions.** Electron localization functions (ELFs) are studied in this part to further reveal the electronic characters for the superatomic bondings discussed above. ELF results indicate electronic density distribution in the cross section of the clusters in color and shape. It is the relative value within the range of (0, 1), in which highest value of 1.0 with red color represents the full delocalization of strong interaction, whereas smallest values of 0.0 with blue color represents no delocalization of the weak interaction.

In order to make the results of ELFs comparable, all Zn clusters $(Zn_4)_2^{n+}$ with different valence electronic numbers $n$ are chosen as the objects in our study to represent the superatomic bonding systems with different bond orders, and their structures are built without optimization to keep the same geometry (the distance between the centers in back faces of two tetrahedral units is 3.18 Å). Specifically, beside $(Zn_4)_2$ with super non bond, $(Zn_4)_2^{2+}$, $(Zn_4)_2^{4+}$ (singlet and triplet), $(Zn_4)_2^{6+}$ are isoelectronic cluster of $(Zn_3Cu)_2$, $(Zn_2Cu_2)_2$ and $(ZnCu_2)_2$ which contain the super single, double, and triple bond, respectively.

The ELF scan is carried on the middle cross section of these clusters as shown in Figure 9. Moreover, the $Ne_2$ with nonbond, $F_2$ with a single bond, $O_2$ (singlet and triplet) with a double bond and $N_2$ with a triple bond are also investigated for comparison. The shape and color of the ELF results indicate the similarity between the simple bonds and the corresponding superatomic bonds with the same bond order. In general, the ELF values increase and the color gradually becomes vivid along with the bond orders, which indicates that the strength of interactions increases. It is worth noting that the shape of the super double bond in singlet and triplet $(Zn_4)_2^{4+}$ has the similar electronic characters as $O_2$. The singlet state is composed of one $\sigma$ bond and one $\pi$ bond, whereas the circular triplet pattern contains one $\sigma$ and two 1/2 three-electron $\pi$ bond exhibiting a magnetic property, of which the latter pattern is more stable. Moreover, the singlet-triplet energy gap of $(Cu_2Zn_2)_2$ is 0.46 eV at PBE0/def2-tzvp level of calculation, and bond energies of singlet and triplet $Cu_2Zn_2$−$Cu_2Zn_2$ cluster are 80.89 and 106.66 kcal/mol, respectively. This result of ELFs confirms the superatomic bonding characters existed in superatomic molecules.

## 3. CONCLUSIONS

In summary, series of Zn−Cu and Mg−Li superatomic molecules with double tetrahedral structures are designed and their bond energies are discussed by density functional

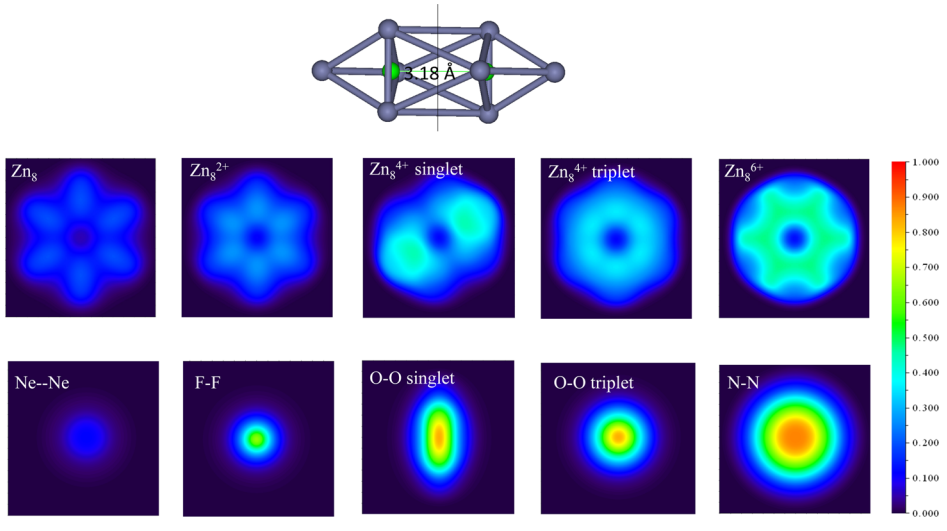


**Figure 9.** ELFs of single bond $(Zn_4)_2^{2+}$, double bond $(Zn_4)_2^{4+}$ (singlet and triplet) and triple bond $(Zn_4)_2^{6+}$ compared with $Ne_2$, $F_2$, $O_2$ (singlet and triplet), and $N_2$ in color and shape. The scale is labeled aside.



DOI: 10.1021/acsomega.8b01841
ACS Omega 2018, 3, 14423−14430

theory (DFT) calculation. Depending on the SVB model, AdNDP analysis reveals that there are super nonbond in 8e−8e $(Zn_4)_2/(Mg_4)_2$, single bond in 7e−7e $(Zn_3Cu)_2/(Mg_3Li)_2$, double bond $(Zn_2Cu_2)_2/(Mg_2Li_2)_2$, and triple bond in 6e−6e $(ZnCu_3)_2/(MgLi_3)_2$, which have the similar characters as the corresponding atomic chemical bonds. Moreover, bond energies are calculated as the key evidence to confirm the bonding characters of these SVBs. The results indicate that the bond energies increase and the bond lengths decrease along with the bond orders in Zn−Cu and Mg−Li systems which is in accordance with the classical nonbond, single bond, double bond, and triple bond in C−H systems. Finally, ELF analysis is carried on to give the direct description for the strength of the electronic interaction to reveal the similarity between the superatomic bonds and the atomic bonds in simple molecules with different bond orders, which confirms the existence of the superatom−superatom bonding systems.

Our study gives the new evidence for the existence of the superatom−superatom bonding depending on bond energies, which would give reference for the further study and design of superatomic clusters.

## 4. COMPUTATIONAL DETAILS

Geometry optimizations and subsequent calculations are performed using DFT methods with PBE0[66,67] functional and relativistic effective core potential basis set (def2-tzvp).[68] The energies of these clusters are also calculated at the PBE0/def2-tzvp level of theory. AdNDP chemical bonding[62−65] and ELF[69−71] analysis is carried on for the optimized geometries to reveal the shape of their chemical bondings at the same level. All the calculations are carried out in the Gaussian 09 package,[72] and the MO visualization is performed using Molekel 5.4.[73]

## AUTHOR INFORMATION


### Corresponding Authors

*E-mail: xuchang_1986@hotmail.com (C.X.).
*E-mail: xiawu@aqnu.edu.cn (X.W.).
*E-mail: clj@ustc.edu (L.C.).

### ORCID

Longjiu Cheng: 0000-0001-7086-6190


### Notes

The authors declare no competing financial interest.

## ACKNOWLEDGMENTS

This work is financed by the National Natural Science Foundation of China (21573001, 21873001), and by the Foundation of Distinguished Young Scientists of Anhui Province. The calculations are carried out at the High-Performance Computing Center of Anhui University.

## REFERENCES


(1) Korzeniewski, G.; Maniv, T.; Metiu, H. The Interaction between an Oscillating Dipole and a Metal Surface Described by a Jellium Model and the Random Phase Approximation. *Chem. Phys. Lett.* **1980**, *73*, 212−217.

(2) de Heer, W. A. The Physics of Simple Metal Clusters: Experimental Aspects and Simple Models. *Rev. Mod. Phys.* **1993**, *65*, 611−676.

(3) Brack, M. The Physics of Simple Metal Clusters: Self-Consistent Jellium Model and Semiclassical Approaches. *Rev. Mod. Phys.* **1993**, *65*, 677−732.

(4) Knight, W. D.; Clemenger, K.; de Heer, W. A.; Saunders, W. A.; Chou, M. Y.; Cohen, M. L. Electronic Shell Structure and Abundances of Sodium Clusters. *Phys. Rev. Lett.* **1984**, *52*, 2141−2143.

(5) Budd, H. F.; Vannimenus, J. Surface Forces and the Jellium Model. *Phys. Rev. Lett.* **1973**, *31*, 1218−1221.

(6) Hartig, J.; Stößer, A.; Hauser, P.; Schnöckel, H. A Metalloid $[Ga_{23}\{N(Sime_3)_2\}_{11}]$ Cluster: The Jellium Model Put to Test. *Angew. Chem., Int. Ed.* **2007**, *46*, 1658−1662.

(7) Melko, J. J.; Clayborne, P. A.; Jones, C. E.; Reveles, J. U.; Gupta, U.; Khanna, S. N.; Castleman, A. W. Combined Experimental and Theoretical Study of $Al_nx$ (N = 1−6; X = as, Sb) Clusters: Evidence of Aromaticity and the Jellium Model. *J. Phys. Chem. A* **2010**, *114*, 2045−2052.

(8) Knight, W. D.; Clemenger, K.; de Heer, W. A.; Saunders, W. A.; Chou, M. Y.; Cohen, M. L. Electronic Shell Structure and Abundances of Sodium Clusters. *Phys. Rev. Lett.* **1984**, *53*, 510.

(9) Liu, Z.; Liu, X.; Zhao, J. Design of Superhalogens Using a Core−Shell Structure Model. *Nanoscale* **2017**, *9*, 18781−18787.

(10) Li, H.-R.; Liu, H.; Tian, X.-X.; Zan, W.-Y.; Mu, Y.-W.; Lu, H.-G.; Li, J.; Wang, Y.-K.; Li, S.-D. Structural Transition in Metal-Centered Boron Clusters: From Tubular Molecular Rotors $Ta@B_{21}$ and $Ta@B_{22}^+$ to Cage-Like Endohedral Metalloborospherene $Ta@B_{22}^-$. *Phys. Chem. Chem. Phys.* **2017**, *19*, 27025−27030.

(11) Li, H.-R.; Liu, H.; Lu, X.-Q.; Zan, W.-Y.; Tian, X.-X.; Lu, H.-G.; Wu, Y.-B.; Mu, Y.-W.; Li, S.-D. Cage-Like $Ta@B_n^q$ Complexes (N = 23−28, Q = −1−+ 3) in 18-Electron Configurations with the Highest Coordination Number of Twenty-Eight. *Nanoscale* **2018**, *10*, 7451−7456.

(12) Luo, Z.; Castleman, A. W.; Khanna, S. N. Reactivity of Metal Clusters. *Chem. Rev.* **2016**, *116*, 14456−14492.

(13) Khanna, S. N.; Jena, P. Assembling Crystals from Clusters. *Phys. Rev. Lett.* **1992**, *69*, 1664−1667.

(14) Mulliken, R. S. The Interpretation of Band Spectra Part Iii. Electron Quantum Numbers and States of Molecules and Their Atoms. *Rev. Mod. Phys.* **1932**, *4*, 1−86.

(15) Tian, Z.; Cheng, L. Electronic and Geometric Structures of $Au_{30}$ Clusters: A Network of 2e-Superatom Au Cores Protected by Tridentate Protecting Motifs with $U_3$-S. *Nanoscale* **2016**, *8*, 826−834.

(16) King, R. B.; Zhao, J. The Isolable Matryoshka Nesting Doll Icosahedral Cluster $[as@Ni_{12}@As_{20}]^{3-}$ as a "Superatom": Analogy with the Jellium Cluster $Al_{13}^-$ Generated in the Gas Phase by Laser Vaporization. *Chem. Commun.* **2006**, 4204−4205.

(17) Huang, X.; Sai, L.; Jiang, X.; Zhao, J. Ground State Structures, Electronic and Optical Properties of Medium-Sized $Na_n^+$ (N = 9, 15, 21, 26, 31, 36, 41, 50 and 59) Clusters from Ab Initio Genetic Algorithm. *Eur. Phys. J. D* **2013**, *67*, 43.

(18) Cheng, L. $B_{14}$: An All-Boron Fullerene. *J. Chem. Phys.* **2012**, *136*, 104301.

(19) Sergeeva, A. P.; Averkiev, B. B.; Zhai, H.-J.; Boldyrev, A. I.; Wang, L.-S. All-Boron Analogues of Aromatic Hydrocarbons: $B_{17}^-$ and $B_{18}^-$. *J. Chem. Phys.* **2011**, *134*, 224304.

(20) Bai, H.; Chen, C.; Zhai, H.-J.; Li, S.-D. Endohedral and Exohedral Metalloborospherenes: $M@B_{40}$ (M=Ca, Sr) and $M\&B_{40}$ (M=Be, Mg). *Angew. Chem., Int. Ed.* **2015**, *54*, 941−945.

(21) Walter, M.; Akola, J.; Lopez-Acevedo, O.; Jadzinsky, P. D.; Calero, G.; Ackerson, C. J.; Whetten, R. L.; Gronbeck, H.; Hakkinen, H. A Unified View of Ligand-Protected Gold Clusters as Superatom Complexes. *Proc. Natl. Acad. Sci. U.S.A.* **2008**, *105*, 9157−9162.

(22) Dhayal, R. S.; Liao, J.-H.; Liu, Y.-C.; Chiang, M.-H.; Kahlal, S.; Saillard, J.-Y.; Liu, C. W. $[Ag_{21}\{S_2p(Oipr)_2\}_{12}]^+$: An Eight-Electron Superatom. *Angew. Chem.* **2015**, *127*, 3773−3777.

(23) Gao, Y.; Liu, X.; Wang, Z. $Ce@Au_{14}$: A Bimetallic Superatom Cluster with 18-Electron Rule. *J. Electron. Mater.* **2017**, *46*, 3899−3903.

(24) Kwak, K.; Tang, Q.; Kim, M.; Jiang, D.-e.; Lee, D. Interconversion between Superatomic 6-Electron and 8-Electron Configurations of $M@Au_{24}(Sr)_{18}$ Clusters (M = Pd, Pt). *J. Am. Chem. Soc.* **2015**, *137*, 10833−10840.




DOI: 10.1021/acsomega.8b01841
*ACS Omega* 2018, 3, 14423−14430

(25) Liao, L.; et al. Structure of Chiral $Au_{44}(2,4\text{-Dmbt})_{26}$ Nanocluster with an 18-Electron Shell Closure. *J. Am. Chem. Soc.* **2016**, *138*, 10425−10428.
(26) Lv, J.; Wang, Y.; Zhang, L.; Lin, H.; Zhao, J.; Ma, Y. Stabilization of Fullerene-Like Boron Cages by Transition Metal Encapsulation. *Nanoscale* **2015**, *7*, 10482−10489.
(27) Zhao, J.; Wang, L.; Li, F.; Chen, Z. $B_{80}$ and Other Medium-Sized Boron Clusters: Core−Shell Structures, Not Hollow Cages. *J. Phys. Chem. A* **2010**, *114*, 9969−9972.
(28) Leuchtner, R. E.; Harms, A. C., Jr.; Castleman, A. W. Thermal Metal Cluster Anion Reactions: Behavior of Aluminum Clusters with Oxygen. *J. Chem. Phys.* **1989**, *91*, 2753−2754.
(29) Reber, A. C.; Khanna, S. N. Superatoms: Electronic and Geometric Effects on Reactivity. *Acc. Chem. Res.* **2017**, *50*, 255−263.
(30) Chen, J.; Luo, Z.; Yao, J. Theoretical Study of Tetrahydrofuran-Stabilized $Al_{13}$ Superatom Cluster. *J. Phys. Chem. A* **2016**, *120*, 3950−3957.
(31) Watanabe, T.; Koyasu, K.; Tsukuda, T. Density Functional Theory Study on Stabilization of the $Al_{13}$ Superatom by Poly(Vinylpyrrolidone). *J. Phys. Chem. C* **2015**, *119*, 10904−10909.
(32) Castleman, A. W.; Khanna, S. N. Clusters, Superatoms, and Building Blocks of New Materials. *J. Phys. Chem. C* **2009**, *113*, 2664−2675.
(33) Bergeron, D. E.; Roach, P. J.; Castleman, A. W.; Jones, N. O.; Khanna, S. N. Al Cluster Superatoms as Halogens in Polyhalides and as Alkaline Earths in Iodide Salts. *Science* **2005**, *307*, 231−235.
(34) Cheng, L.; Yang, J. Communication: New Insight into Electronic Shells of Metal Clusters: Analogues of Simple Molecules. *J. Chem. Phys.* **2013**, *138*, 141101.
(35) Yuan, Y.; Cheng, L.; Yang, J. Electronic Stability of Phosphine-Protected $Au_{20}$ Nanocluster: Superatomic Bonding. *J. Phys. Chem. C* **2013**, *117*, 13276−13282.
(36) Wang, H.; Cheng, L. Quintuple Super Bonding between the Superatoms of Metallic Clusters. *Nanoscale* **2017**, *9*, 13209−13213.
(37) Koyasu, K.; Tsukuda, T. A Face-Sharing Bi-Icosahedral Model for $Al_{23}^-$. *Phys. Chem. Chem. Phys.* **2014**, *16*, 21717−21720.
(38) Liu, L.; Li, P.; Yuan, L.-F.; Cheng, L.; Yang, J. From Isosuperatoms to Isosupermolecules: New Concepts in Cluster Science. *Nanoscale* **2016**, *8*, 12787−12792.
(39) Cheng, L.; Ren, C.; Zhang, X.; Yang, J. New Insight into the Electronic Shell of $Au_{38}(Sr)_{24}$: A Superatomic Molecule. *Nanoscale* **2013**, *5*, 1475−1478.
(40) Wan, X.-K.; Lin, Z.-W.; Wang, Q.-M. $Au_{20}$ Nanocluster Protected by Hemilabile Phosphines. *J. Am. Chem. Soc.* **2012**, *134*, 14750−14752.
(41) Das, A.; Li, T.; Nobusada, K.; Zeng, Q.; Rosi, N. L.; Jin, R. Total Structure and Optical Properties of a Phosphine/Thiolate-Protected $Au_{24}$ Nanocluster. *J. Am. Chem. Soc.* **2012**, *134*, 20286−20289.
(42) Liang, X.-Q.; Deng, X.-J.; Lu, S.-J.; Huang, X.-M.; Zhao, J.-J.; Xu, H.-G.; Zheng, W.-J.; Zeng, X. C. Probing Structural, Electronic, and Magnetic Properties of Iron-Doped Semiconductor Clusters $Fe_2ge_n^{-/0}$ (N = 3−12) Via Joint Photoelectron Spectroscopy and Density Functional Study. *J. Phys. Chem. C* **2017**, *121*, 7037−7046.
(43) Whoolery, A. J.; Dahl, L. F. Synthesis and Structural-Bonding Analysis of the $[Au_6ni_{12}(Co)_{24}]^{2-}$ Dianion Containing an Unprecedented 18-Vertex Cubic Td Metal Core Composed of Five Face-Fused Octahedra: The First Example of a Discrete Gold/Nickel Bimetallic-Bonded Species. *J. Am. Chem. Soc.* **1991**, *113*, 6683−6685.
(44) Muñoz-Castro, A. $Sp^3$-Hybridization in Superatomic Clusters. Analogues to Simple Molecules Involving the Au6 Core. *Chem. Sci.* **2014**, *5*, 4749−4754.
(45) Muñoz-Castro, A.; King, R. B. Au102+ and Au6X42+ clusters: Superatomic Molecules Bearing an $Sp^3$-Hybrid $Au_6$ Core. *Int. J. Quantum Chem.* **2017**, *117*, No. e25331.
(46) Muñoz-Castro, A. $D_{6h}$-$Au_{42}$ Isomer: A Golden Aromatic Toroid Involving Superatomic Π-Orbitals Which Follows the Hückel (4*n*+2) Rule. *ChemPhysChem* **2016**, *17*, 3204−3208.
(47) Li, J.; Li, X.; Zhai, H.-J.; Wang, L.-S. Au20: A Tetrahedral Cluster. *Science* **2003**, *299*, 864−867.
(48) King, R. B.; Chen, Z.; Schleyer, P. v. R. Structure and Bonding in the Omnicapped Truncated Tetrahedral Au20 Cluster: Analogies between Gold and Carbon Cluster Chemistry. *Inorg. Chem.* **2004**, *43*, 4564−4566.
(49) Cheng, L.; Zhang, X.; Jin, B.; Yang, J. Superatom−Atom Super-Bonding in Metallic Clusters: A New Look to the Mystery of an $Au_{20}$ Pyramid. *Nanoscale* **2014**, *6*, 12440−12444.
(50) Ren, L.; Cheng, L. Structural Prediction of $(Au_{20})_N$ (N=2−40) Clusters and Their Building-up Principle. *Comput. Theor. Chem.* **2012**, *984*, 142−147.
(51) Zubarev, D. Y.; Boldyrev, A. I. Deciphering Chemical Bonding in Golden Cages. *J. Phys. Chem. A* **2009**, *113*, 866−868.
(52) Muñoz-Castro, A.; Saillard, J.-Y. Cover Feature: $[Au_{12}(Sr)_6]^{2-}$, as Smaller 8-Electron Gold Nanocluster Retaining an $Sp^3$-Core. Evaluation of Bonding and Optical Properties from Relativistic Dft Calculations. *ChemPhysChem* **2018**, *19*, 1800.
(53) Pei, Y.; Lin, S.; Su, J.; Liu, C. Structure Prediction of $Au_{44}(Sr)_{28}$: A Chiral Superatom Cluster. *J. Am. Chem. Soc.* **2013**, *135*, 19060−19063.
(54) Pei, Y.; Tang, J.; Tang, X.; Huang, Y.; Zeng, X. C. New Structure Model of $Au_{22}(Sr)_{18}$: Bitetrahederon Golden Kernel Enclosed by $[Au_6(Sr)_6]$ Au(I) Complex. *J. Phys. Chem. Lett.* **2015**, *6*, 1390−1395.
(55) Pei, Y.; Gao, Y.; Shao, N.; Zeng, X. C. Thiolate-Protected $Au_{20}(Sr)_{16}$ Cluster: Prolate Au8 Core with New $[Au_3(Sr)_4]$ Staple Motif. *J. Am. Chem. Soc.* **2009**, *131*, 13619−13621.
(56) Dong, H.; Liao, L.; Zhuang, S.; Yao, C.; Chen, J.; Tian, S.; Zhu, M.; Liu, X.; Li, L.; Wu, Z. A Novel Double-Helical-Kernel Evolution Pattern of Gold Nanoclusters: Alternate Single-Stranded Growth at Both Ends. *Nanoscale* **2017**, *9*, 3742−3746.
(57) Liu, L.; Yuan, J.; Cheng, L.; Yang, J. New Insights into the Stability and Structural Evolution of Some Gold Nanoclusters. *Nanoscale* **2017**, *9*, 856−861.
(58) Tian, Z.; Cheng, L. Perspectives on the Energy Landscape of Au-Cl Binary Systems from the Structural Phase Diagram of $Au_xcl_y$ (X + Y = 20). *Phys. Chem. Chem. Phys.* **2015**, *17*, 13421−13428.
(59) Yan, L.; Cheng, L.; Yang, J. Tetrahedral $Au_{17}^+$: A Superatomic Molecule with a $Au_{13}$ Fcc Core. *J. Phys. Chem. C* **2015**, *119*, 23274−23278.
(60) Cheng, L.; Cai, W.; Shao, X. A Conformational Analysis Method for Understanding the Energy Landscapes of Clusters. *ChemPhysChem* **2007**, *8*, 569−577.
(61) Yan, L.-j.; Cheng, L.-j.; Yang, J.-l. $Sp^3$-Hybridization Feature of $Ag_4$ Superatom in Superatomic Molecules. *Chin. J. Phys.* **2015**, *28*, 476−480.
(62) Zubarev, D. Y.; Boldyrev, A. I. Developing Paradigms of Chemical Bonding: Adaptive Natural Density Partitioning. *Phys. Chem. Chem. Phys.* **2008**, *10*, 5207−5217.
(63) Hay, P. J.; Wadt, W. R. Ab Initio Effective Core Potentials for Molecular Calculations. Potentials for the Transition Metal Atoms Sc to Hg. *J. Chem. Phys.* **1985**, *82*, 270−283.
(64) Zubarev, D. Y.; Boldyrev, A. I. Comprehensive Analysis of Chemical Bonding in Boron Clusters. *J. Comput. Chem.* **2007**, *28*, 251−268.
(65) Zubarev, D. Y.; Boldyrev, A. I. Revealing Intuitively Assessable Chemical Bonding Patterns in Organic Aromatic Molecules Via Adaptive Natural Density Partitioning. *J. Org. Chem.* **2008**, *73*, 9251−9258.
(66) Perdew, J. P.; Burke, K.; Ernzerhof, M. Generalized Gradient Approximation Made Simple. *Phys. Rev. Lett.* **1996**, *77*, 3865−3868.
(67) Perdew, J. P.; Burke, K.; Wang, Y. Generalized Gradient Approximation for the Exchange-Correlation Hole of a Many-Electron System. *Phys. Rev. B: Condens. Matter Mater. Phys.* **1996**, *54*, 16533−16539.
(68) Weigend, F.; Ahlrichs, R. Balanced Basis Sets of Split Valence, Triple Zeta Valence and Quadruple Zeta Valence Quality for H to Rn:


DOI: 10.1021/acsomega.8b01841
*ACS Omega* 2018, 3, 14423−14430

Design and Assessment of Accuracy. *Phys. Chem. Chem. Phys.* **2005**, *7*, 3297−3305.
(69) Schmider, H. L.; Becke, A. D. Chemical Content of the Kinetic Energy Density. *J. Mol. Struct.: THEOCHEM* **2000**, *527*, 51−61.
(70) Burdett, J. K.; McCormick, T. A. Electron Localization in Molecules and Solids: The Meaning of Elf. *J. Phys. Chem. A* **1998**, *102*, 6366−6372.
(71) Savin, A.; Nesper, R.; Wengert, S.; Fässler, T. F. Elf: The Electron Localization Function. *Angew. Chem. Int. Ed.* **1997**, *36*, 1808−1832.
(72) Frisch, M. J.; Trucks, G. W.; Schlegel, H. B.; Scuseria, G.; Robb, M.; Cheeseman, J.; Scalmani, G.; Barone, V.; Mennucci, B.; Petersson, G.; et al. *Gaussian 09*, Revision B.01; Gaussian, Inc.: Wallingford, CT, 2009.
(73) Varetto, U. *Molekel*, version 5.4. 0.8; Swiss National Supercomputing Centre: Manno, Switzerland, 2009.



DOI: 10.1021/acsomega.8b01841
*ACS Omega* 2018, 3, 14423−14430